# Three-dimensional spectrally encoded imaging

**D. Yelin, B. E. Bouma, N. Iftimia, and G. J. Tearney**

*Harvard Medical School and the Wellman Laboratories of Photomedicine, Massachusetts General Hospital, 55 Fruit Street, BAR 703, Boston, Massachusetts 02114*

Received June 17, 2003

A method for three-dimensional surface measurements with phase-sensitive spectrally encoded imaging is demonstrated. Both transverse and depth information is transmitted through a single-mode optical fiber, allowing this scheme to be incorporated into a miniature probe. This approach is demonstrated by measurement of the profile of a lens surface and by three-dimensional imaging of the face of a small doll. © 2003 Optical Society of America

*OCIS codes:* 120.6660, 170.6900, 110.6150, 170.4580.

Optical techniques for surface profilometry are commonly performed with interferometric measurements. Analyzing the interference fringe pattern formed by overlap of a reflected wave from an optically smooth surface with a reference wave permits surface profile measurements with high accuracy.[1] Projecting an interference fringe pattern on an object surface is effective for probing rough surfaces.[2] High-resolution, point-by-point measurements of rough surfaces have been demonstrated by use of a long coherence length source with a Fizeau interferometer[3] and with a broadband source.[4,5] White-light interferometry is capable of simultaneously imaging a large field of view by scanning only the path length of the reference arm.[6] In this approach, light reflected from the surface interferes with a reference wave to form a speckle pattern on a camera. When the reference optical path length is scanned, each individual speckle exhibits an intensity modulation. The surface height is determined at the maximum point of the modulation envelope. White-light interferometry is an extremely robust technique, allowing for high-resolution imaging in three dimensions with a large field of view.

Depth-resolved imaging with a large, three-dimensional (3-D) field of view is more challenging when one is utilizing small-diameter flexible imaging probes such as borescopes, laparoscopes, and endoscopes. Confocal imaging through a fiber bundle with a lens with a high numerical aperture[7] is one solution to this problem. The 3-D field of view for these devices, however, is limited to less than a few millimeters because of the small objective lens's clear aperture and the low $f$-number required for high-resolution optical sectioning. Other methods, such as stereo imaging[8] and structured illumination,[9] have been proposed. These methods all require additional hardware for the probe, increasing the size, cost, and complexity of these devices. Recently, a method for performing a miniature endoscopy with a high number of resolvable points was presented.[10] This approach uses a broadband light source and a diffraction grating to spectrally encode reflectance across a transverse line within the sample. A two-dimensional (2-D) image is formed by slowly scanning this spectrally encoded line. Since this method requires only a single optical fiber, it permits 2-D imaging through a small-diameter, flexible probe.

In this Letter we describe a phase-sensitive spectrally encoded imaging scheme that, in addition to providing 2-D images of a specimen, is also capable of measuring surface profiles. This additional information is obtained without altering the probe. In 3-D spectrally encoded imaging, the transverse location of the image is encoded by wavelength, and the axial or depth coordinate of each point is encoded by phase. A schematic of the system is shown in Fig. 1. A broadbandwidth titanium–sapphire (center wavelength 860 nm, 200-nm FWHM bandwidth) was coupled into the input port of a single-mode fiber-optic 50/50 Michelson interferometer. At the sample arm, a diffraction grating (600 lines/mm) was used to disperse the spectrum in the horizontal image plane ($x$ axis). A lens ($f$ = 75 mm, beam diameter 1 mm) focused the individual spectrally encoded points onto the specimen. The beam was scanned in the vertical dimension ($y$ axis) by a galvanometric scanner (60 Hz) to create a 2-D image. These parameters resulted in a spatial transverse resolution of approximately 40 $\mu$m. The image was composed of approximately 585 × 585 resolvable points; each transverse spot contained a bandwidth of 0.34 nm. The overall power on the sample was 10 mW.

To obtain surface profiles, we controlled the path length of the reference arm by moving a mirror mounted on a translation stage. The power of the reference beam was attenuated by use of a neutral-density filter to maximize the contrast of the interference pattern. At the detection arm, the fields from the sample and reference arms were combined and spatially dispersed by a diffraction grating (600 lines/mm) and a lens ($f$ = 60 mm) onto a CCD

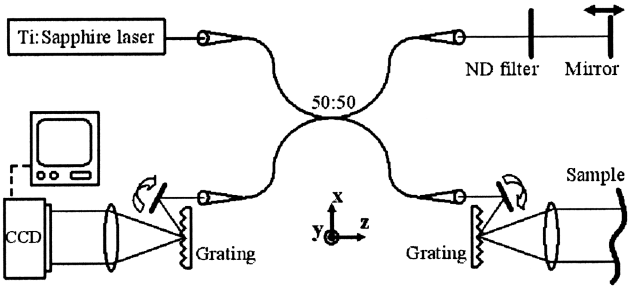


Fig. 1. Schematic of the 3-D spectrally encoded imaging system. ND, neutral density.

0146-9592/03/232321-03$15.00/0 

array. Vertical scanning was performed by another galvanometric scanner that was synchronized with the sample-arm $y$-axis scanner. The resulting interference pattern was viewed on a monitor in real time, digitized, and stored.

At each horizontal line on the CCD, the intensity is given by

$$I(\omega) = |E(\omega) + E_0(\omega)|^2 = 2|A_0(\omega)|^2\{1 - \cos[\phi(\omega) - \phi_0(\omega)]\}, \quad (1)$$

where $E(\omega) = A(\omega)\exp[i\phi(\omega)]$ and $E_0(\omega) = A_0(\omega) \times \exp[i\phi_0(\omega)]$ are the spectra reflected from the sample and the reference arms, respectively. For simplicity, we assume that the spectral amplitudes from the sample and reference arms are real and equal, $A(\omega) = A_0(\omega)$. Algorithms for extracting phase difference from a spectral interference signal between two waves with continuous and smooth phases are well known. Spectral phase measurements were performed mainly for dispersion measurements with broadband sources[11] and white light.[12] By use of a Fourier-limited reference field [$\phi_0(\omega) = 0$] with a given delay $\tau$ between the reference and the signal fields, the interference term in Eq. (1) is simply $\cos[\phi(\omega) - \omega\tau]$. With a straightforward algorithm,[13] the spectral phase can be unambiguously extracted from the interference pattern $I(\omega)$. In our configuration the surface height $h$ at each point is given by $h = c\phi(\omega)/(2\omega)$, where $c$ is the speed of light.

To demonstrate the ability of this scheme to probe optically smooth surfaces, we placed a plano–convex lens (Melles-Griot, $f = 1$ m, BK7 glass), with its convex surface facing toward the grating, in the sample arm. To match the optical path length over the entire field of view, an additional two lenses, in a confocal configuration, were placed at the sample arm between the scanner and the diffraction grating. A delay of 2.18 ps (654 $\mu$m) was introduced between the sample and the reference arms. The interference pattern for this setup is shown in Fig. 2a. The measured surface profile along a horizontal line in Fig. 2a, obtained with the algorithm described by Lepetit *et al.*,[13] is plotted as a solid curve in Fig. 2b, with the calculated lens's radius (dashed curve). The differences between the measured and the calculated profiles can be attributed to the loss of fringe contrast on the right-hand side of the frame and to low fringe density on the left-hand side. When the sample contained steep local slopes, the fringe pattern became too dense to be resolved by our imaging system. This limitation prevented our system from measuring optically smooth surfaces with slopes greater than $\lambda/d$, where $\lambda$ is the wavelength and $d$ is the transverse spot size.

In most industrial and medical applications the specimen surface is not optically smooth but contains many surface irregularities. When the surface is rough and the diffraction-limited point-spread function of the imaging system is broad compared with the microscopic surface variations, the interference between the sample and the reference is manifested by a granular speckle pattern. This pattern has a characteristic speckle size that matches the system's point-spread function. The depth of the speckle pattern along the $z$ axis is defined by the coherence length, CL $\cong cN/\Delta\omega$, where $N$ is the number of resolvable points along the $x$ axis (wavelength) and $\Delta\omega$ is the total source bandwidth. Unlike white-light interferometry, where the coherence length CL is given by $c/\Delta\omega$ and can be as short as a few micrometers, here the coherence length is $N$ times larger, since it is determined by only the spectral width of each spectrally encoded spot. Throughout this work, the coherence length (310 $\mu$m) was smaller than the confocal parameter (2.7 mm) and therefore determined the axial resolution. The large depth of focus allowed imaging over a range equivalent to the confocal parameter by scanning only the optical path length of the reference arm.

To demonstrate the ability of our 3-D spectrally encoded imaging apparatus to measure the profile of rough surfaces, we imaged the face of a small plastic doll. The doll's face is shown in Fig. 3a. The standard spectrally encoded 2-D image was obtained by blocking the reference arm[10] (Fig. 3b). When the light returned from the reference arm was allowed to interfere with that of the sample arm, a speckle pattern was observed in portions of the image. A full 3-D data set was acquired by capturing 45 frames as the reference-arm path length was scanned in steps of 100 $\mu$m. The natural logarithm of the absolute value of the difference between consecutive frames was calculated, followed by moderate volumetric smoothing (the kernel is $3 \times 3 \times 3$ pixels). We obtained the

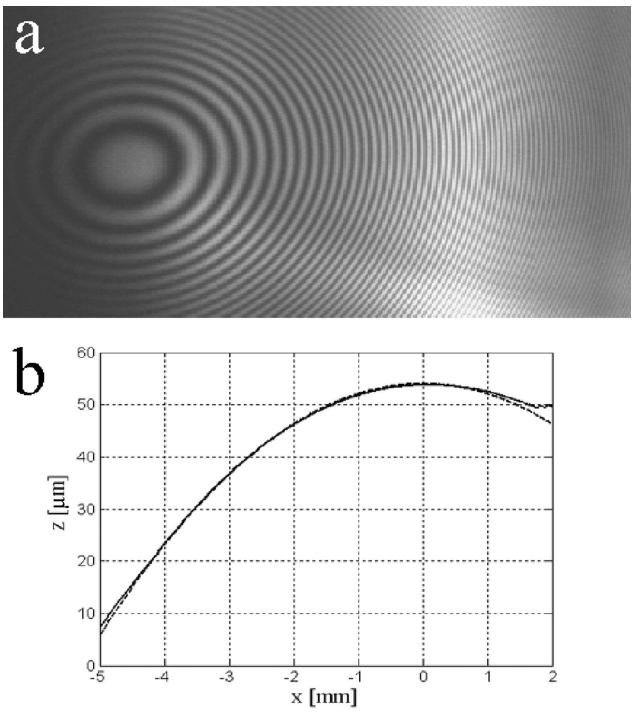


Fig. 2. a, 2-D spectrally encoded interferogram from the curved surface of a lens ($f = 1$ m). b, Profile of the lens (solid curve) measured with our setup agrees with the calculated profile (dashed curve).

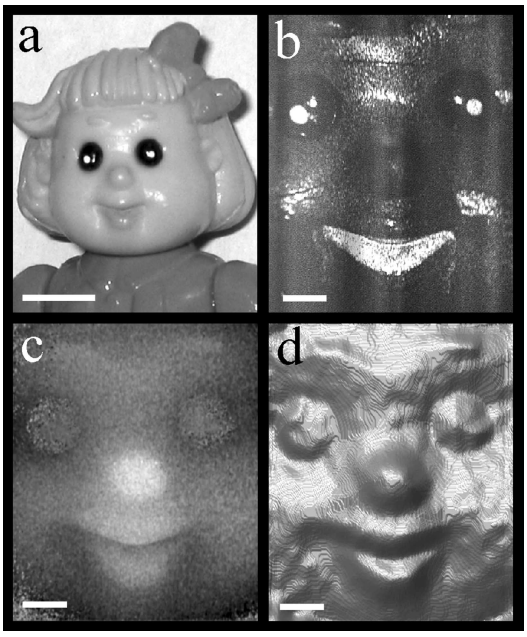


Fig. 3. 3-D imaging of a doll's face. a, Image of the doll's face obtained with white-light illumination and a standard CCD camera (scale bar 4 mm). b, 2-D spectrally encoded image obtained with the reference arm blocked. c, The surface height, measured by 3-D spectrally encoded imaging, is represented as a gray-scale image, where $z$ values closer to the probe have a higher pixel intensity. d, Surface rendering of the data shown in Fig. 3c. The scale bars in b–d represent 1 mm.

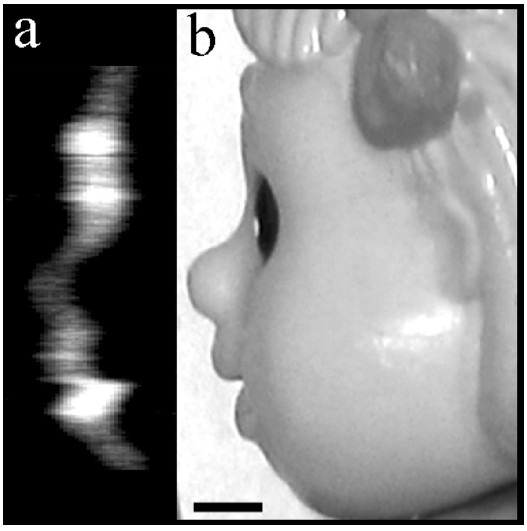


Fig. 4. a, $y-z$ (saggital) section from the middle of the processed data volume adjacent to b, a standard CCD image of the doll's profile (scale bar 1 mm).

surface height by determining the location of the maximum speckle intensity difference along the axial ($z$) axis (displayed as a gray-scale image in Fig. 3c). The doll's face can also be represented by surface 3-D rendering (Fig. 3d). For estimating the experimental depth resolution we plotted a sagittal ($y-z$) section from this data set (Fig. 4a) next to the actual doll's profile (Fig. 4b). Our measurement revealed an axial resolution of approximately 330 $\mu$m (FWHM of the coherence envelope), which is in reasonable agreement with the predicted axial resolution of 310 $\mu$m.

3-D spectrally encoded imaging can be used in many configurations to suit specific applications. For example, this method is capable of measuring a surface within a volume of 50 mm $\times$ 50 mm $\times$ 30 mm ($x$, $y$, $z$, respectively) with, typically, 200 $\times$ 200 $\times$ 280 resolution points. Using a fast CCD camera and a rapidly scanning optical delay line in the reference arm,[14] one could capture the 3-D data set and display it in real time (30 frames/s).

This study was funded in part by the Center for Integration of Medicine and Innovative Technology, a National Science Foundation grant (BES-0086709), and the Whitaker Foundation, and through a generous gift from Dr. and Mrs. J. S. Chen to the optical diagnostics program of the Massachusetts General Hospital Wellman Laboratories of Photomedicine. D. Yelin's e-mail address is dyelin@partners.org.

## References

1. Y. Y. Cheng and J. C. Wyant, Appl. Opt. **24,** 804 (1985).
2. B. C. Kim and S. W. Kim, Opt. Lett. **28,** 528 (2003).
3. D. P. Hand, T. A. Carolan, J. S. Barton, and J. D. C. Jones, Opt. Lett. **18,** 1361 (1993).
4. P. J. Caber, Appl. Opt. **32,** 3438 (1993).
5. A. V. Zvyagin, I. Eix, and D. D. Sampson, Appl. Opt. **41,** 2179 (2002).
6. T. Dresel, G. Häusler, and H. Venzke, Appl. Opt. **31,** 919 (1992).
7. Y. S. Sabharwal, A. R. Rouse, L. Donaldson, M. F. Hopkins, and A. F. Gmitro, Appl. Opt. **38,** 7133 (1999).
8. M. Chan, W. Lin, C. Zhou, and J. Y. Qu, Appl. Opt. **42,** 1888 (2003).
9. D. Karadaglic, R. Juskaitis, and T. Wilson, Proc. SPIE **4964,** 84 (2003).
10. G. J. Tearney, M. Shishkov, and B. E. Bouma, Opt. Lett. **27,** 412 (2002).
11. W. H. Knox, Appl. Phys. B **58,** 225 (1994).
12. A. P. Kovács, K. Osvey, Zs. Bor, and R. Szipöcs, Opt. Lett. **20,** 788 (1995).
13. L. Lepetit, G. Chériaux, and M. Joffre, J. Opt. Soc. Am. B **12,** 2467 (1995).
14. K. K. M. B. D. Silva, A. V. Zvyagin, and D. D. Sampson, Electron. Lett. **35,** 1404 (1999).